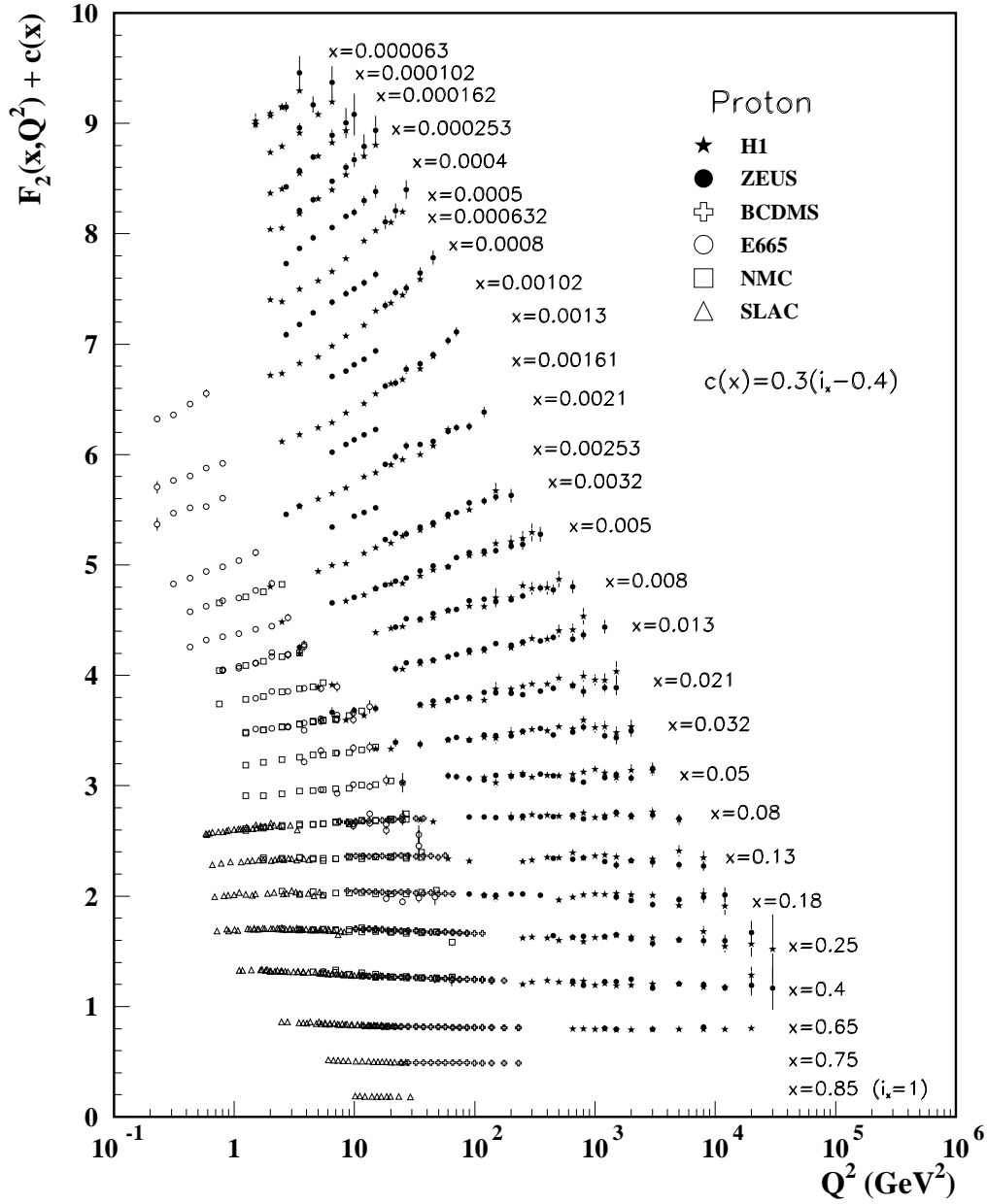
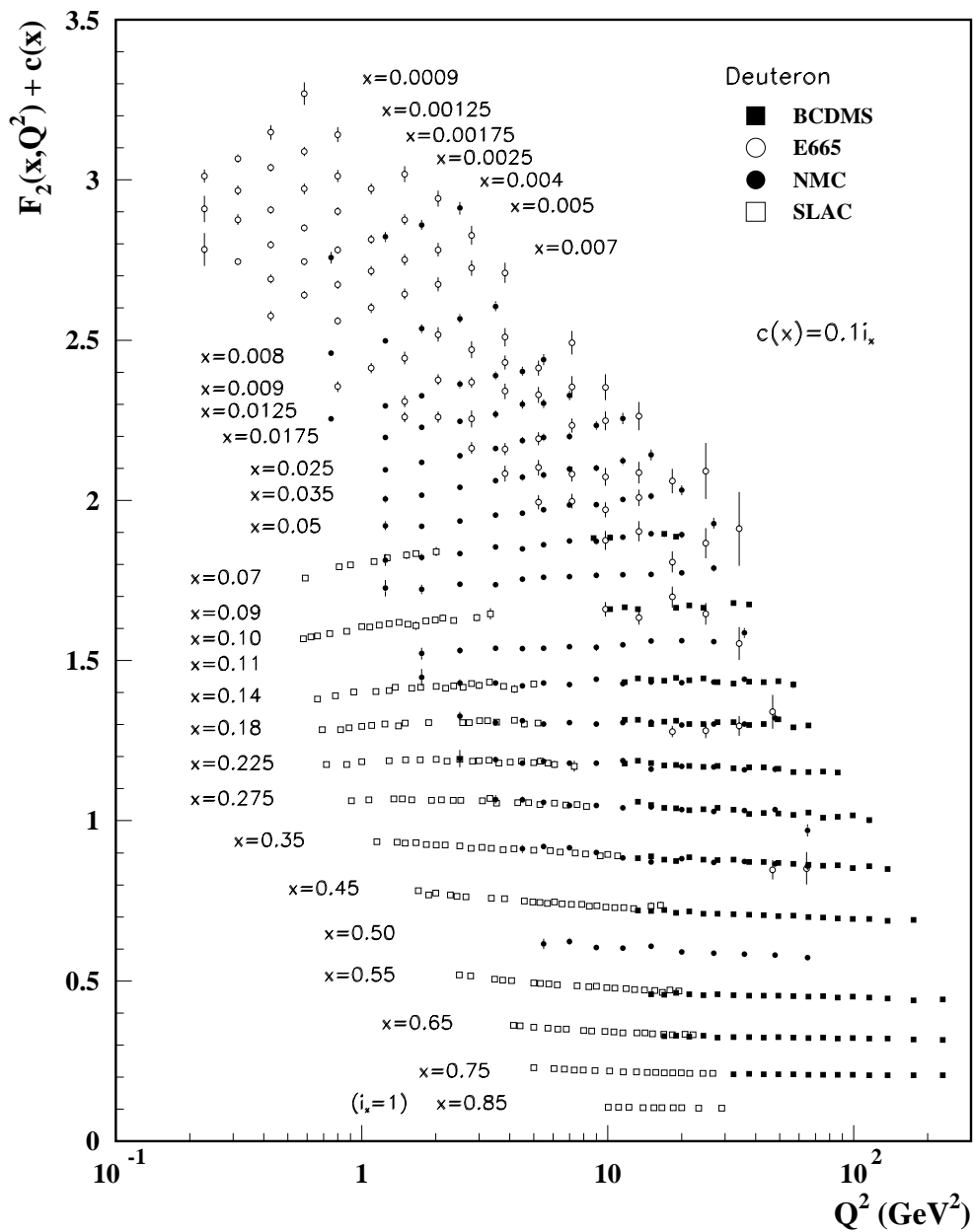


NOTE: THE FIGURES IN THIS SECTION ARE INTENDED TO SHOW THE REPRESENTATIVE DATA. THEY ARE NOT MEANT TO BE COMPLETE COMPILATIONS OF ALL THE WORLD'S RELIABLE DATA.



**Figure 14.6:** The proton structure function  $F_2^p$  measured in electromagnetic scattering of positrons on protons (collider experiments ZEUS and H1), in the kinematic domain of the HERA data, for  $x > 0.00006$  (cf. Fig. 14.9 for data at smaller  $x$  and  $Q^2$ ), and for electrons (SLAC) and muons (BCDMS, E665, NMC) on a fixed target. Statistical and systematic errors added in quadrature are shown. The data are plotted as a function of  $Q^2$  in bins of fixed  $x$ . The ZEUS binning in  $x$  is used in this plot; all other data are rebinned to the  $x$  values of the ZEUS data. For the purpose of plotting, a constant  $c(x) = 0.3(i_x - 0.4)$  is added to  $F_2^p$ , where  $i_x$  is the number of the  $x$  bin ranging from  $i_x = 1$  ( $x = 0.85$ ) to  $i_x = 28$  ( $x = 0.000063$ ). References: **H1**—C. Adloff *et al.*, *Eur. Phys. J.* **C21**, 33 (2001); C. Adloff *et al.*, *Eur. Phys. J.* **C13**, 609 (2000); **ZEUS**—S. Chekanov *et al.*, *Eur. Phys. J.* **C21**, 443 (2001); **BCDMS**—A.C. Benvenuti *et al.*, *Phys. Lett.* **B223**, 485 (1989) (as given in [46]); **E665**—M.R. Adams *et al.*, *Phys. Rev.* **D54**, 3006 (1996); **NMC**—M. Arneodo *et al.*, *Nucl. Phys.* **B483**, 3 (97); **SLAC**—L.W. Whitlow *et al.*, *Phys. Lett.* **B282**, 475 (1992).



**Figure 14.7:** The deuteron structure function  $F_2^d$  measured in electromagnetic scattering of electrons (SLAC) and muons (BCDMS, E665, NMC) on a fixed target, shown as a function of  $Q^2$  for bins of fixed  $x$ . Statistical and systematic errors added in quadrature are shown. For the purpose of plotting, a constant  $c(x) = 0.1i_x$  is added to  $F_2^d$  where  $i_x$  is the number of the  $x$  bin, ranging from 1 ( $x = 0.85$ ) to 29 ( $x = 0.0009$ ). References: **BCDMS**—A.C. Benvenuti *et al.*, Phys. Lett. **B237**, 592 (1990). **E665**, **NMC**, **SLAC**—same references as Fig. 14.6.

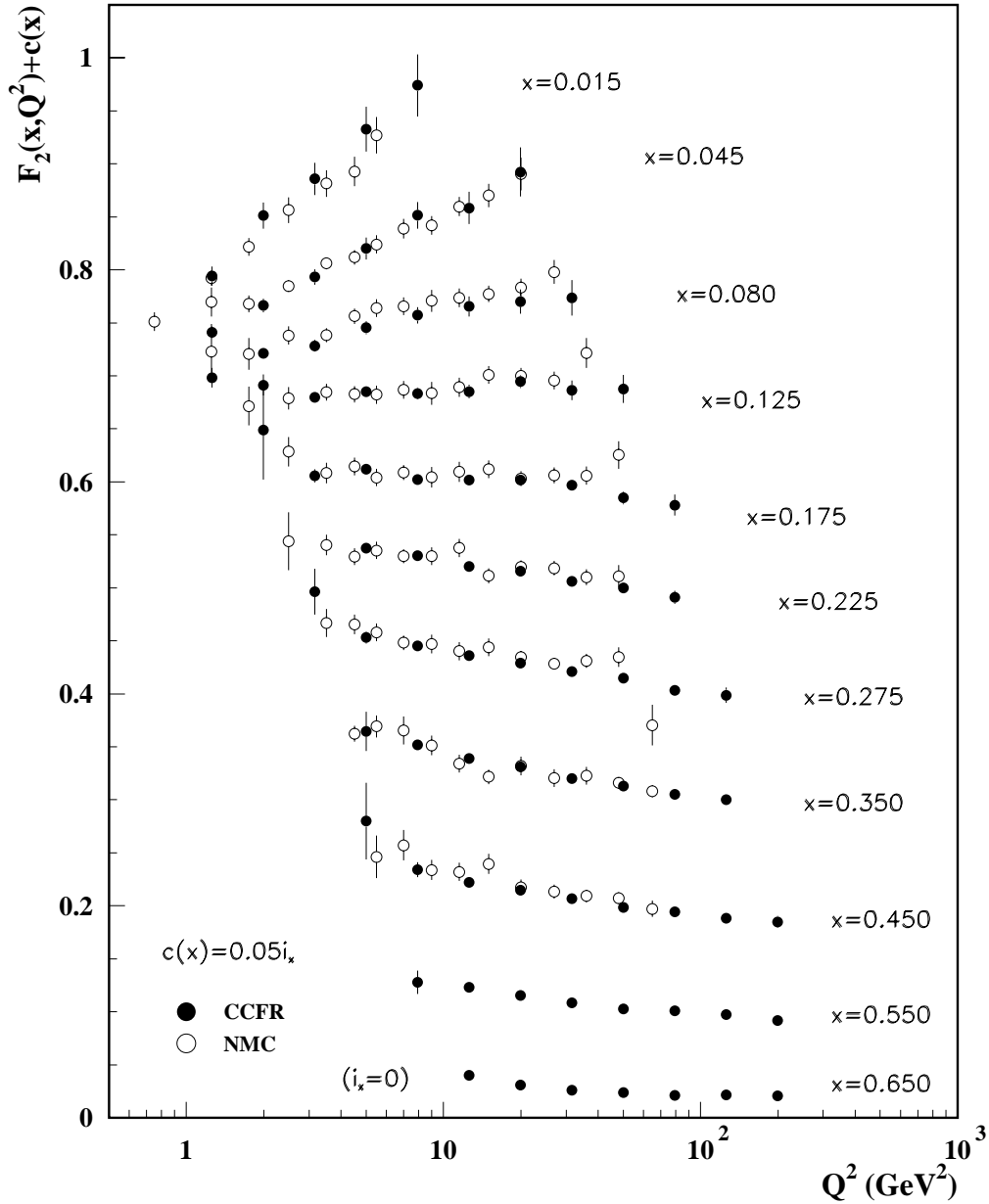


**Figure 14.8:** The deuteron structure function  $F_2$  measured in deep inelastic scattering of muons on a fixed target (NMC) is compared to the structure function  $F_2$  from neutrino-iron scattering (CCFR) using  $F_2^\mu = (5/18)F_2^\nu - x(s + \bar{s})/6$ , where heavy target effects have been taken into account. The data are shown versus  $Q^2$ , for bins of fixed  $x$ . The NMC data have been rebinned to CCFR  $x$  values. Statistical and systematic errors added in quadrature are shown. For the purpose of plotting, a constant  $c(x) = 0.05i_x$  is added to  $F_2$  where  $i_x$  is the number of the  $x$  bin, ranging from 0 ( $x = 0.65$ ) to 10 ( $x = 0.015$ ). References: NMC—M. Arneodo *et al.*, Nucl. Phys. **B483**, 3 (97); CCFR/NuTeV—U.K. Yang *et al.*, Phys. Rev. Lett. **86**, 2741 (2001).

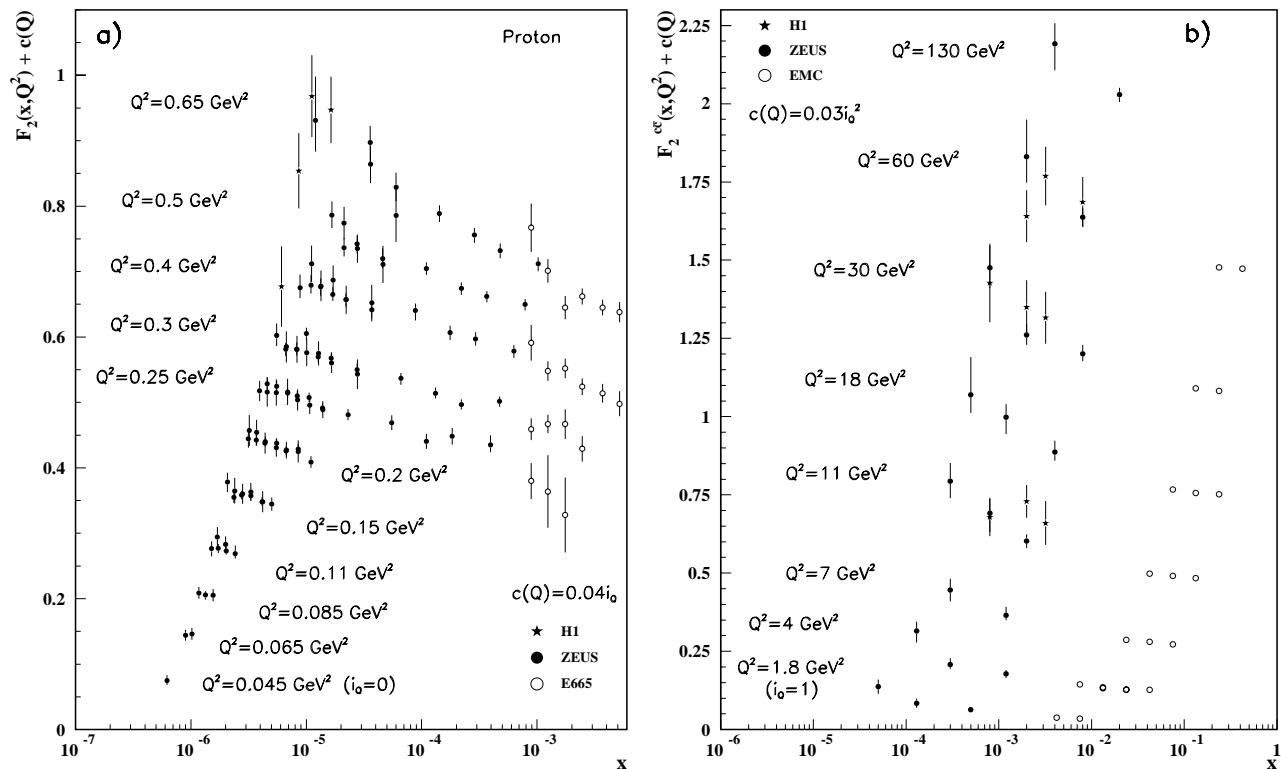


**Figure 14.9:** a) The proton structure function  $F_2^p$  at small  $x$  and  $Q^2$ , measured in electromagnetic scattering of positrons (H1, ZEUS) and muons (E665) on protons. For the purpose of plotting, a constant  $c(Q) = 0.04i_Q$  is added to  $F_2^p$  where  $i_Q$  is the number of the  $Q^2$  bin, ranging from 0 ( $Q^2 = 0.045 \text{ GeV}^2$ ) to 10 ( $Q^2 = 0.65 \text{ GeV}^2$ ). References: **ZEUS**—J. Breitweg *et al.*, Phys. Lett. **B407**, 432 (1997); J. Breitweg *et al.*, Phys. Lett. **B487**, 53 (2000); J. Breitweg *et al.*, Eur. Phys. J. **C7**, 609 (1999); **H1**—C. Adloff *et al.*, Nucl. Phys. **B497**, 3 (1997); **E665**—M.R. Adams *et al.*, Phys. Rev. **D54**, 3006 (1996).

b) The charm structure function  $F_2^{c\bar{c}}(x)$ , i.e. that part of the inclusive structure function  $F_2^p$  arising from the production of charm quarks, measured in electromagnetic scattering of positrons on protons (H1, ZEUS) and muons on iron (EMC). For the purpose of plotting, a constant  $c(Q) = 0.03i_Q^2$  is added to  $F_2^{c\bar{c}}$  where  $i_Q$  is the number of the  $Q^2$  bin, ranging from 1 ( $Q^2 = 1.8 \text{ GeV}^2$ ) to 8 ( $Q^2 = 130 \text{ GeV}^2$ ). References: **ZEUS**—J. Breitweg *et al.*, Eur. Phys. J. **C12**, 35 (2000); **H1**—C. Adloff *et al.*, Z. Phys. **C72**, 593 (1996); **EMC**—J.J. Aubert *et al.*, Nucl. Phys. **B213**, 31 (1983).

Statistical and systematic errors added in quadrature are shown for both plots. The data are given as a function of  $x$  in bins of  $Q^2$ .

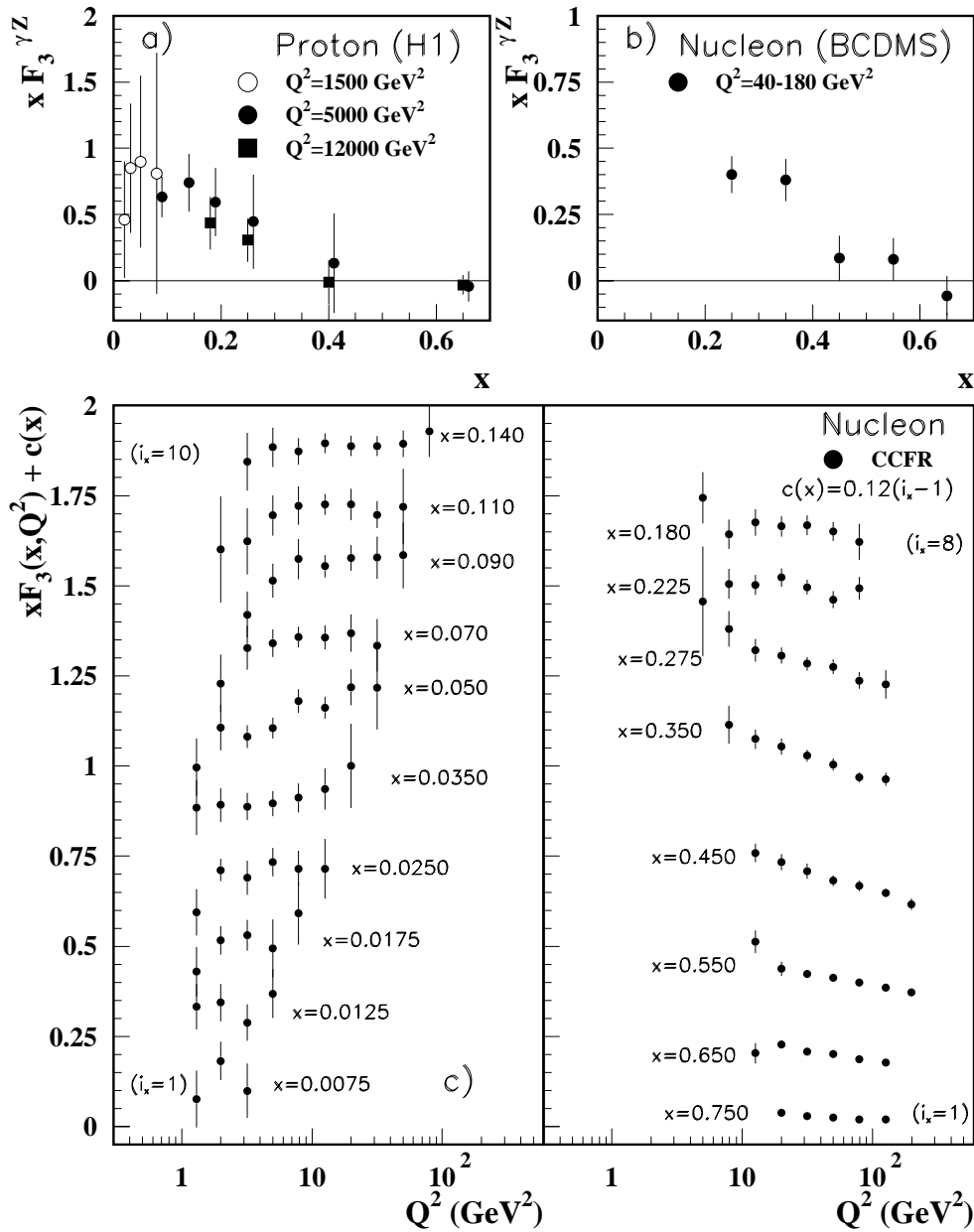


**Figure 14.10:** The structure function  $x F_3^{\gamma Z}$  measured in electroweak scattering of a) electrons on protons (H1) and b) muons on carbon (BCDMS). Statistical and systematic errors added in quadrature are shown. References: **H1**—C. Adloff *et al.*, Eur. Phys. J. **C19**, 269 (2001); **BCDMS**—A. Argento *et al.*, Phys. Lett. **B140**, 142 (1984).

c) The structure function  $x F_3$  of the nucleon measured in  $\nu$ -Fe scattering. Statistical and systematic errors added in quadrature are shown. The data are plotted as a function of  $Q^2$  in bins of fixed  $x$ . For the purpose of plotting, a constant  $c(x) = 0.12(i_x - 1)$  is added to  $x F_3$ , where  $i_x$  is the number of the  $x$  bin as shown in the plot. References: **CCFR**—W. G. Seligman *et al.*, Phys. Rev. Lett. **79**, 1213 (1997).

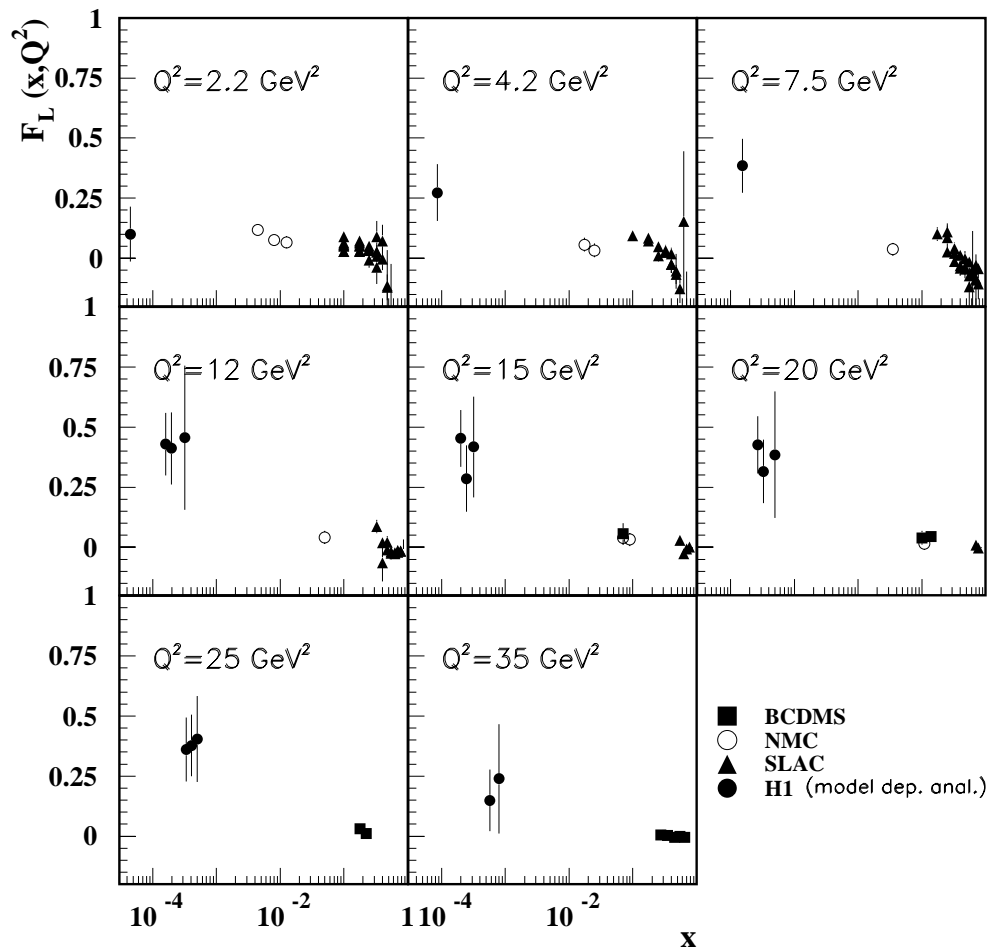


**Figure 14.11:** The longitudinal structure function  $F_L$  as a function of  $x$  in bins of fixed  $Q^2$  measured on the proton (except for the SLAC data which also contain deuterium data). The H1 result requires the assumption of the validity of the QCD form for the  $F_2$  structure function in order to extract  $F_L$ . BCDMS, NMC, and SLAC results are from measurements of  $R$  (the ratio of longitudinal to transverse photon absorption cross sections) which are converted to  $F_L$  by using the BCDMS parameterization of  $F_2$  (A.C. Benvenuti *et al.*, Phys. Lett. **B223**, 485 (1989)). It is assumed that the  $Q^2$  dependence of the fix-target data is small within a given  $Q^2$  bin. Statistical and systematic errors added in quadrature are shown. References: H1—C. Adloff *et al.*, Eur. Phys. J. **C21**, 33 (2001); BCDMS—A. Benvenuti *et al.*, Phys. Lett. **B223**, 485 (1989); NMC—M. Arneodo *et al.*, Nucl. Phys. **B483**, 3 (1997); SLAC—L.W. Whitlow *et al.*, Phys. Lett. **B250**, 193 (1990) and numerical values from the thesis of L.W. Whitlow (SLAC-357).

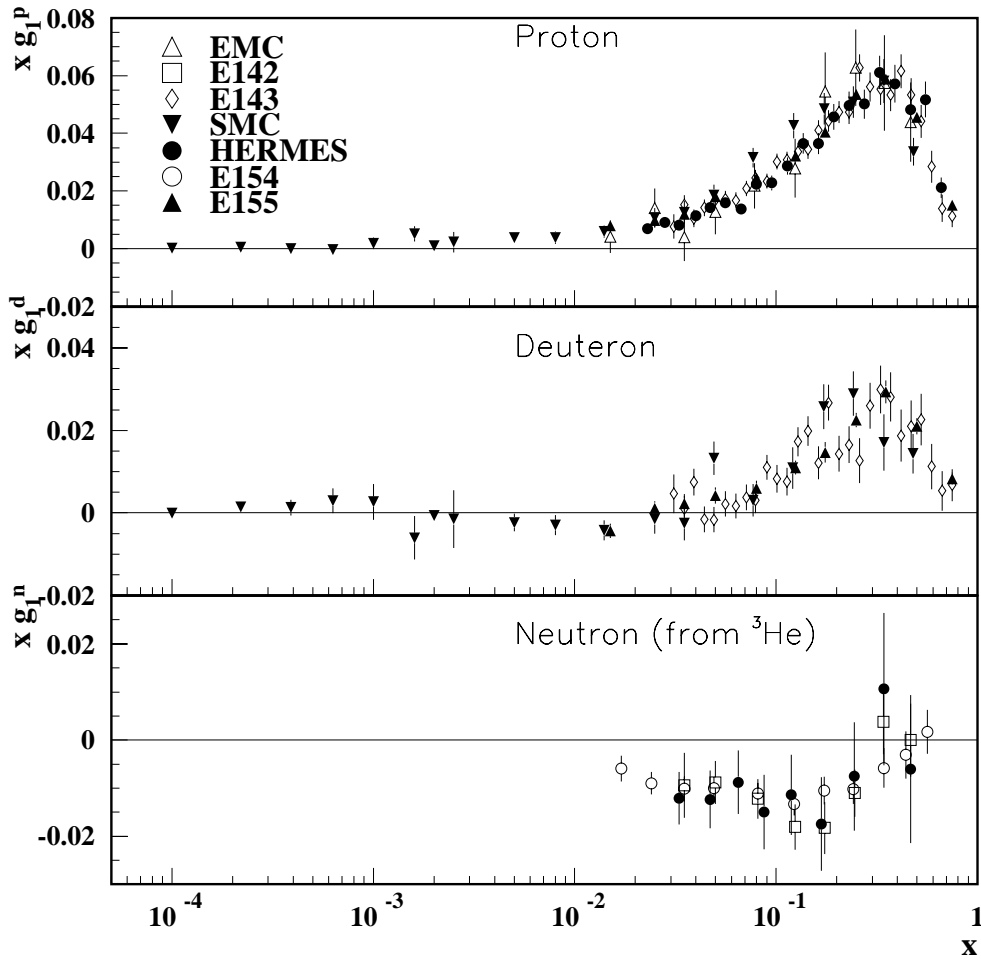


**Figure 14.12:** The spin-dependent structure function  $xg_1(x)$  of the proton, deuteron, and neutron (from  $^3\text{He}$  target) measured in deep inelastic scattering of polarized electrons/positrons: E142 ( $Q^2 \sim 0.3 - 10 \text{ GeV}^2$ ), E143 ( $Q^2 \sim 0.3 - 10 \text{ GeV}^2$ ), E154 ( $Q^2 \sim 1 - 17 \text{ GeV}^2$ ), E155 ( $Q^2 \sim 1 - 40 \text{ GeV}^2$ ), HERMES ( $Q^2 \sim 0.8 - 20 \text{ GeV}^2$ ) and muons: EMC ( $Q^2 \sim 1.5 - 100 \text{ GeV}^2$ ), SMC ( $Q^2 \sim 0.01 - 100 \text{ GeV}^2$ ), shown at the measured  $Q^2$  (except for EMC data given  $Q^2 = 10.7 \text{ GeV}^2$  and E155 data given at  $Q^2 = 5 \text{ GeV}^2$ ). Note that  $g_1^n(x)$  may also be extracted by taking the difference between  $g_1^d(x)$  and  $g_1^p(x)$ , but these values have been omitted in the bottom plot for clarity. Statistical and systematic errors added in quadrature are shown. References: **EMC**—J. Ashman *et al.*, Nucl. Phys. **B328**, 1 (1989); **E142**—P.L. Anthony *et al.*, Phys. Rev. **D54**, 6620 (1996); **E143**—K. Abe *et al.*, Phys. Rev. **D58**, 112003 (1998); **SMC**—B. Adeva *et al.*, Phys. Rev. **D58**, 112001 (1998), B. Adeva *et al.*, Phys. Rev. **D60**, 072004 (1999) and Erratum-Phys. Rev. **D62**, 079902 (2000); **HERMES**—A. Airapetian *et al.*, Phys. Lett. **B442**, 484 (1998) and K. Ackerstaff *et al.*, Phys. Lett. **B404**, 383 (1997); **E154**—K. Abe *et al.*, Phys. Rev. Lett. **79**, 26 (1997); **E155**—P.L. Anthony *et al.*, Phys. Lett. **B463**, 339 (1999) and P.L. Anthony *et al.*, Phys. Lett. **B493**, 19 (2000).